Impacts that pH and metal ion concentration have on the synthesis of bimetallic and trimetallic nanorods from gold seeds†

Zusing Yang, Yang-Wei Lin, Wei-Lung Tseng and Huan-Tsung Chang*

Received 7th January 2005, Accepted 25th April 2005
First published as an Advance Article on the web 12th May 2005
DOI: 10.1039/b500256g

This paper describes the synthesis of Au–Ag bimetallic and Au–Ag–Hg trimetallic nanorods (NRs) from gold NRs, which acted as seeds, under alkaline conditions (pH $\geqslant$ 8.0) and in the presence of hexadecyltrimethylammonium bromide (CTAB), ascorbic acid, and other metal ions. The Hg^{2+}, Fe^{3+}, and Co^{2+} ions are stable at pH $\geqslant$ 8.5 in the presence of 200 mM glycine; these conditions allow investigations into their roles during the syntheses of the NRs. We prepared a number of differently colored NRs by controlling the pH and the nature and concentration of the metal ion. Mercury ions, which have a higher reduction potential and form a more stable complex with glycine, are reduced and deposited on the gold NRs to form Au–Ag–Hg trimetallic NRs; we confirmed this situation by performing inductively coupled plasma-mass spectrometry and energy dispersive X-ray measurements. In addition, we have demonstrated that the size and shape of the Au–Ag–Hg trimetallic NRs can be tuned by controlling the Hg^{2+} concentration.

Introduction

Nanostructured materials, such as gold nanorods (NRs), are used in various fields, including sensors, catalysis, and surface-enhanced Raman scattering, because of their large surface areas and characteristic optical and electrical properties.[1,2] One striking feature of gold NRs is that their optical properties depend on their shapes and aspect ratios (length : width ratios), which can be controlled by using templates and gold seeds.[3,4] Core–shell and alloyed multimetallic nanoparticles (NPs) that have optical and catalytic properties that differ from those of their individual constituent metals are also of interest and importance in both theoretical and applied science.[5] In addition to their shapes and aspect ratios, the optical properties of metal NPs and nanorods (NRs) also depend on the ratio of their metal components,[5b,c,6] the thickness of their shells,[7] and their extinction coefficients.[5b] For example, seeding methods have been used to synthesize differently shaped Au_{core}–Ag_{shell} NRs that have high extinction coefficients for their surface plasmon resonance (SPR) absorbance in the near infrared region.[5a,7c,8] By controlling the silver ion concentration and the ratio of the gold and silver ions, Au_{core}–Ag_{shell} NRs having different sizes and shapes have been synthesized in the presence of ascorbic acid ($pK_{a1,2}$ = 4.1, 11.8) under alkaline conditions.[5a,9] These previous studies have highlighted the important role that the cationic surfactant, hexadecyltrimethylammonium bromide (CTAB),[3,4c,10] plays in controlling the shapes and sizes of the Au_{core}–Ag_{shell} gold NRs.[5a,8,9c] Because of the adsorption of CTAB micelles on the gold surface,[10a] the Ag atoms that are reduced by ascorbate under alkaline conditions are deposited selectively on the {111} facets of the gold NRs.[4e,11] Recently, we have used gold NRs as seeds to prepare high-quality (purity > 90%) dumbbell-shaped Au_{core}–Ag_{shell} NRs in glycine solutions (pH > 8.0).[9c] We have found that the pH controls the reducing ability of ascorbic acid and the reduction potentials of the gold and silver ions and, thus, it is an important parameter for controlling the size, shape, and purity of the Au_{core}–Ag_{shell} NRs. The prepared Au_{core}–Ag_{shell} NRs are stable for > 3 months in glycine solutions.

In this paper, we describe an extension of our study to further investigate the effects that metal ions have on the synthesis of Au_{core}–Ag_{shell} NRs. Our hypothesis was that the metal ions might decrease the reducing ability of ascorbic acid—through the formation of complexes with it—and alter the reaction pathways in systems in which redox reactions could occur between two different metal ions and/or metal ions and ascorbate. Thus, we expected to form different types of NPs when using gold NRs as seeds in the presence of various metal ions. Indeed, in the presence of mercury ions, we synthesized Au–Ag–Hg trimetallic NRs.

Experimental

Chemicals

Silver nitrate, sodium tetrachloroaurate dehydrate, and sodium borohydride were purchased from Aldrich (Milwaukee, WI, USA). Hexadecyltrimethylammonium bromide and potassium dichromate(VI) were purchased from Acros (Geel, Belgium). Glycine was purchased from MP Biomedicals, Inc (Irvine, CA, USA). L-Ascorbic acid, mercury(II) chloride, and potassium ferricyanide(III) were purchased from J. T. Baker (Phillipsburg, NJ, USA). Cobalt(II) nitrate was purchased from Merck (Whitehouse Station, NJ, USA). Milli-Q ultrapure water was used in all experiments.

† Electronic supplementary information (ESI) available: TEM images for gold nanorods and TEM images and UV-vis spectra fro Au–Ag nanrods prepared from gold seeds in the presence of Co^{2+} and Fe^{2+}. See http://www.rsc.org/suppdata/jm/b5/b500256g/

*changht@ntu.edu.tw

Synthesis of gold NRs

Gold NRs were synthesized by using a seed-mediated growth method.[4d] In a typical procedure, the seed solution was prepared by first mixing CTAB (0.2 M, 5 mL) with $NaAuCl_4$ (0.5 mM, 5 mL) and then adding ice-cold $NaBH_4$ (0.01 M, 0.6 mL). The color of the solution changed from dark yellow to brownish yellow under vigorous stirring, indicating the formation of the seed solution. In a separate flask, CTAB (0.2 M, 5.0 mL), $NaAuCl_4$ (1.0 mM, 5.0 mL), and $AgNO_3$ (4.0 mM, 0.25 mL) were mixed. Under vigorous stirring, ascorbic acid (AA, 78.8 mM, 70 μL) was added to the as-prepared solution, causing the solution's color to change from dark yellow to colorless. Finally, a portion of the seed solution (12 μL) was added to the colorless solution. The resulting solution was incubated overnight (>12 h) until the color changed from colorless to red, indicating the formation of gold NR solution. The longitudinal SPR absorbance of the as-prepared gold NRs was located at 841 nm; their aspect ratio was *ca.* 3.61 (see Fig. S1 in the Electronic Supplementary Information (ESI)†). We note that some ascorbic acid, gold ions, and silver ions remained in this gold NR solution.

Synthesis of bimetallic and trimetallic NRs

The gold NR solutions that acted as growth solutions were used directly for the preparation of bimetallic and trimetallic NRs.[4d] Aliquots of the growth solution (1.0 mL) were mixed with 500 mM glycine solutions (pH 8.0, 9.5, and 10.5; 0.8 mL) that were adjusted with NaOH and then with deionized water (0.2 mL) to bring their final volumes to 2.0 mL. The resulting solutions were incubated overnight (>12 h).

To investigate the role that the metal ion plays during the formation of the Au–Ag NRs, we selectively chose to study Fe^{3+}, Co^{2+}, and Hg^{2+} ions. Aliquots of the growth solution (1.0 mL), 500 mM glycine solutions (pH 8.0, 9.5, and 10.5; 0.8 mL), and 0.01 M Fe^{3+}, Co^{2+}, or Hg^{2+} aqueous solution (0.02 mL) were mixed. These mixtures were then diluted with deionized water to bring their final volumes to 2.0 mL. The resulting solutions were incubated overnight (>12 h).

Absorbance and transmission electron microscopy (TEM) measurements

A double-beam UV–vis spectrophotometer (Cintra 10e) obtained from GBC (Victoria, Australia) was used to measure the extinction of the prepared solutions. The TEM images were recorded using a JEOL JSM-1200EX II TEM (JEOL Ltd., Akishima, Japan), operating at 100 kV. For TEM measurements, the as-prepared nanoparticles were subjected to two centrifuge–wash cycles to remove excess CTAB; centrifugation was conducted at 12 000 rpm for 15 min and deionized water (2.0 mL) was used for washing in each cycle. For TEM measurements, the nanoparticles were deposited on a TEM grid coated with a thin layer of carbon. Energy-dispersive X-ray (EDX) measurements were performed using a Philips Tecnai 20 G2 S-Twin microscope (Philips Ltd., Holland) operating at 300 kV.

Results and discussion

We monitored the evolution of the NR-formation process in the different mixtures by performing UV–vis absorbance measurements. Increases in the extinction and greater blue-shifts of the longitudinal SPR are evidence for the deposition of Ag^+ onto the gold NRs.[5a,7c,9] It has been reported that these changes are related to the "effective" dielectric constants of the different thicknesses of the silver coatings, the formation of the Au–Ag interface,[5b] and the aspect ratio of the Au_{core}–Ag_{shell} NRs.[5a–c,9c] Because of the low reduction potentials of Fe^{3+} (Fe^{3+}/Fe^{2+} *vs.* NHE, $E^0 = 0.771$ V) and Co^{2+} (Co^{2+}/Co *vs.* NHE, $E^0 = -0.282$ V) relative to that of Ag^+ (Ag^+/Ag *vs.* NHE, $E^0 = 0.791$ V), no redox reactions occur between Ag^0 and Fe^{3+} or Co^{2+}. We confirmed this assumption by considering the fact that no deposition of these two metals occurred on the Au–Ag NRs when measuring them by ICP-MS.[9c,12] The formation of complexes between the metal ions and Br^- ions can be ignored because they have much lower stabilities than the ones formed between the metal ions and either glycine or ascorbate. Because these metal ions form complexes with ascorbate, albeit weak ones, they decrease the reducing ability of ascorbate for the reduction of Ag^+.[13] This hypothesis is supported by the slower increases in the intensity and blue shift in the longitudinal SPR absorbance of the mixture containing Fe^{3+} (826 nm, pH 8.0; 799 nm, pH 9.5; 794 nm, pH 10.5) relative to those containing Co^{2+} (750 nm, pH 8.0; 681 nm, pH 9.5; 652 nm, pH 10.5); this finding indicates that the deposition of silver onto the gold NRs occurs to a lesser extent in the former case because of the greater stability of the Fe^{3+}–ascorbate complex relative to that of the Co^{2+}–ascorbate complex (see Figs. S2 and S3 in the ESI†).[13c] We note that only slight changes occurred in the as-prepared gold NRs (after three wash–centrifuge cycles) when we increased the value of the pH from 3.0 to 10.5. In the presence of silver ions and ascorbate, however, differently shaped and sized Au–Ag NRs can be prepared.[9c] In that previous study, we highlighted the fact that glycine formed complexes with Au^+ and Ag^+ such that precipitation of AgBr and AgCl was prevented and their oxidizing strengths were reduced.

Fig. 1a presents the trends of increased SPR absorbances and shifts in the longitudinal SPR (>700 nm) that occurred upon increasing the aging time in the presence of Hg^{2+} (Hg^{2+}/Hg *vs.* NHE, $E^0 = 0.852$ V) at pH 8.0. During the first 90 min of the reaction, the longitudinal SPR absorbance increased gradually and underwent a red shift; these observations indicate that deposition of Au and Ag occurs on the gold NRs.[5a,b,7c,9] The residual Au^+ (Au^{3+}) and Ag^+ in the gold NR solution were reduced further by ascorbate at high pH.[4d,9c] In contrast, during the reaction period from 120 to 180 min, the longitudinal SPR absorbance decreased and underwent a blue shift, which indicates that the deposition of Hg occurred onto the gold NRs at pH 8.0.[6c,14,15] The decrease in the longitudinal SPR absorbance after the deposition of Hg onto the gold NRs is likely to be due to the lower "average" dielectric constant when compared to that of the Au–Ag NRs.[5b,14] The deposition of Au, Ag, and Hg is further supported by the results of inductively coupled plasma mass spectrometry (ICP-MS) measurements (Table 1). The deposition of Ag and Hg occurred

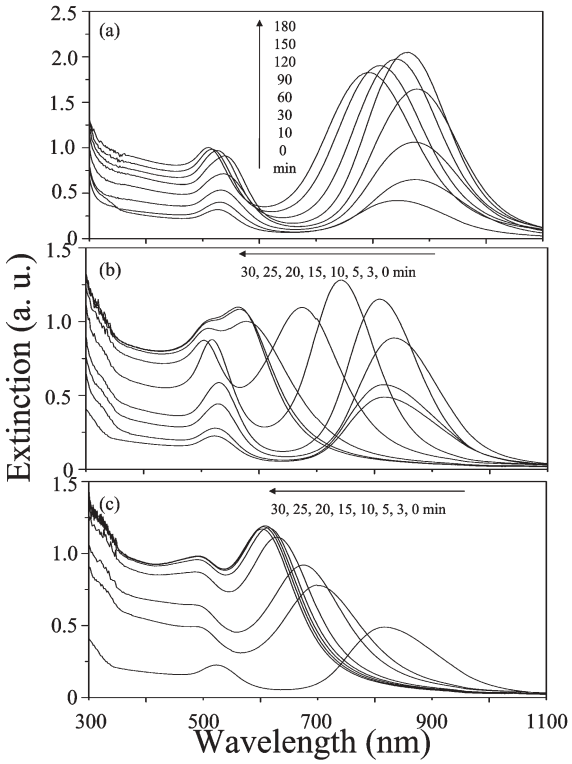

Fig. 1 UV–vis absorption spectra, plotted as a function of time, for the mixtures containing 10^{-4} M Hg^{2+} at pH (a) 8.0, (b) 9.5, and (c) 10.5.

Table 1 Ratios of elemental abundances as measured by ICP-MS for the Au–Ag–Hg trimetallic NRs[a]

Time/min	[Ag]/[Au]	[Hg]/[Au]
0	—	—
30	0.007	—
60	0.012	—
90	0.024	—
120	0.054	—
150	0.061	0.003
180	0.070	0.008

[a] The NRs were dissolved in aqueous 2% HNO_3 solutions prior to ICP-MS analysis.

separately after *ca.* 30 and 150 min, respectively. The ICP-MS data and the changes in the SPR bands reveal a time dependence for the deposition of Au, Ag, and Hg, which indicates that the sizes and shapes of the gold NRs might change upon the deposition of these metals. We note that the amount of Au^0 increased with time, which suggests the formation of alloys.[5]

Although Hg^{2+} possesses a higher reduction potential than does Ag^+, it was reduced by ascorbate after its reduction of Ag^+, mainly because Hg^{2+} ions form stronger complexes with glycine (log K_f = 20.1) than do Ag^+ ions (log K_f = 6.9).[16] The formation of glycine complexes also prevents the formation of $HgCl_2$ and AgCl precipitates. We note that the systems reached their equilibria after longer periods of time when in the presence of Hg^{2+} (>180 min) than they did when in the presence of Co^{2+} (60 min) and Fe^{3+} (90 min). Fig. 1 also

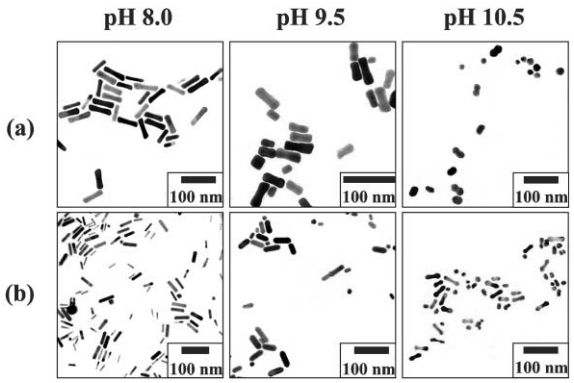

Fig. 2 TEM images of the as-prepared NRs synthesized (a) in the absence and (b) in the presence of Hg^{2+}. All other conditions are the same as those used to obtain Fig. 1.

displays the UV–vis spectra of the growth solutions containing Hg^{2+} at pH 9.5 and 10.5 during the course of the reaction from 0–30 min; these spectra indicate that a faster reaction occurred at higher pH as a result of the stronger reducing ability of ascorbate under such conditions.[13] The three sets of spectra in Fig. 1 indicate that different NPs formed at the different values of pH.

We recorded transmission electron microscopy (TEM, Hitachi, H-7100) images to provide direct evidence that different NRs formed in the presence of Hg^{2+} at the various values of pH. The TEM images depicted in Fig. 2 confirm that the as-prepared NRs are different when synthesized in the absence and presence of Hg^{2+}. The aspect ratios of the as-prepared NRs were 3.39, 2.89, and 4.10 at pH 8.0, 9.5, and 10.5, respectively; these values differ from those obtained in the absence of Hg^{2+} (4.10, 2.72, and 1.90, respectively). The presence of Hg in the NRs is supported by the data from ICP-MS measurements; the percentages of Hg were 4.1, 4.1, and 7.7% at pH 8.0, 9.5, and 10.5, respectively. These results infer that we had formed Au–Ag–Hg trimetallic composites. Table 2 lists a more detailed comparison of the physical and optical properties of the Au–Ag bimetallic and Au–Ag–Hg trimetallic NRs. We note that the sizes of the Au–Ag–Hg trimetallic NRs are smaller than those at pH 3.0; this situation is likely to be due to dissolution of the two ends of the gold NRs, mainly because CTAB formed ion pairs with chloride ions (>0.01 M). The Au–Ag bimetallic NRs prepared in the presence of Co^{2+} and Fe^{3+} were also smaller than those formed in the absence of

Table 2 Physical and optical properties of Au–Ag bimetallic and Au–Ag–Hg trimetallic NRs

pH	Metal ion	Length/nm	Width/nm	λ_T/nm[a]	λ_L/nm[b]
8.0	—	58 ± 7	14 ± 2	525	740
	Hg^{2+}	36 ± 10	11 ± 2	502	792
9.5	—	43 ± 8	16 ± 1	525	740
	Hg^{2+}	43 ± 6	15 ± 2	507	634
10.5	—	34 ± 4	20 ± 2	516	—
	Hg^{2+}	36 ± 6	11 ± 2	487	756
3.0[c]	—	53 ± 5	15 ± 1	524	841

[a] λ_T represents the transverse SPR absorbance of the NRs. [b] λ_L represents the longitudinal SPR absorbance of the NRs. [c] These data refer to the gold NRs prepared at pH 3.0.

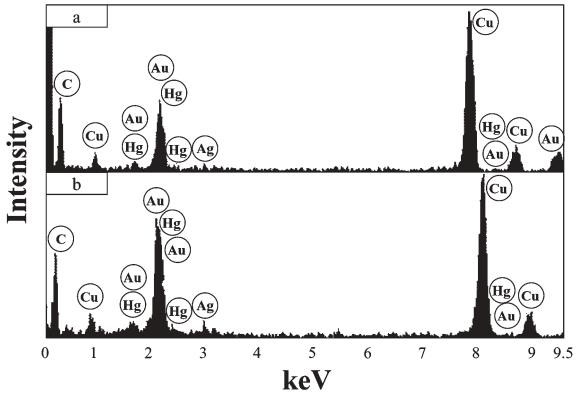

Fig. 3 EDX spectra for the as-prepared Au–Ag–Hg trimetallic NRs prepared at pH 8.0. The beam was focused on a single NR (a) at its center and (b) on its side. The size of the beam was 5.0 nm; for correction, half of the beam was focused on a single NR and the other half on the carbon matrix.

the two metal ions. For example, the sizes of the Au–Ag bimetallic NRs that we prepared at pH 8.0 in the absence of Co^{2+} and Fe^{3+} were 58 $\pm$ 7 nm, whereas those formed in the presence of Co^{2+} and Fe^{3+} had sizes of 49 $\pm$ 6 and 35 $\pm$ 5 nm, respectively. Thus, the ionic strength (*i.e.*, the concentration of counter ions) seems to play a role in determining the sizes and shapes of the NRs.

The energy dispersive X-ray (EDX) measurements (Fig. 3) reveal that the percentages of Au, Ag, and Hg in the Au–Ag–Hg trimetallic NRs (pH 8.0) were 87.7, 7.8, and 4.4%, respectively; these values are in agreement with those obtained from the ICP-MS measurements. As revealed in Fig. 3b, the percentages of Au, Ag, and Hg on the surface (a 5 nm beam was focused on the side of a single NR) of the Au–Ag–Hg trimetallic NRs were 86.3, 8.8, and 4.9%, respectively. These results suggest that a Au–Ag–Hg trimetallic alloy formed on the surface.

Our hypothesis is also supported by the changes that occurred—as evidenced from TEM images—in the sizes and shapes of the NRs during the course of the first 150 min of the reaction. Fig. 4 indicates that the lengths and widths of the Au–Ag–Hg trimetallic NRs decreased upon increasing the aging time; the lengths (widths) were 51 $\pm$ 5 (13 $\pm$ 2) and 38 $\pm$ 7 (11 $\pm$ 2) nm after reaction times of 30 and 150 min, respectively. Because Hg^{2+} is involved in the formation of the Au–Ag–Hg trimetallic NRs, its concentration should affect the physical and optical properties of the NRs. When we increased

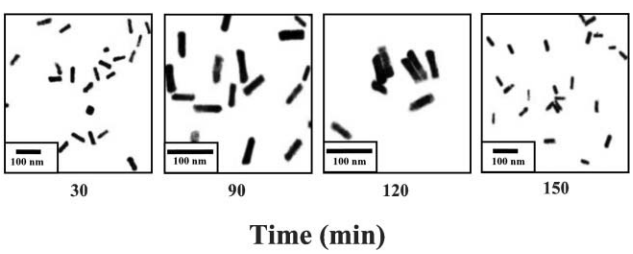

Fig. 4 TEM images obtained as a function of time for the as-prepared Au–Ag–Hg trimetallic NRs synthesized in the presence of 10^{-4} M Hg^{2+} at pH 8.0.

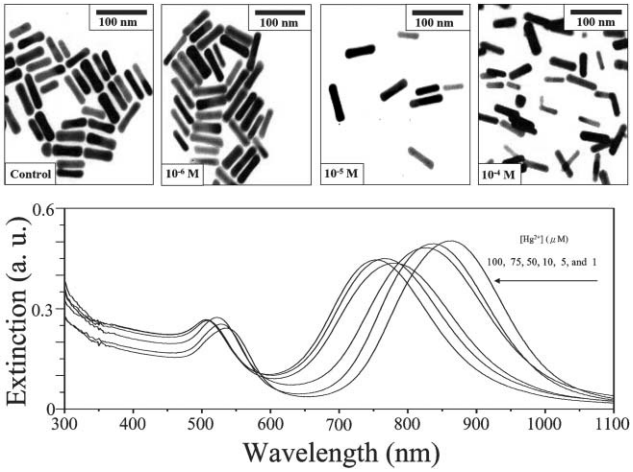

Fig. 5 TEM images and UV spectra of the Au–Ag–Hg trimetallic NRs prepared at pH 8.0 in the presence of different concentrations of Hg^{2+}.

the concentration of Hg^{2+}, the sizes of the Au–Ag–Hg trimetallic NRs decreased and their longitudinal SPR band underwent a blue shift, as indicated in Fig. 5. The colors varied from pink to brown when we changed the Hg^{2+} concentration from 1 to 100 μM.

In summary, we have demonstrated that the presence of metal ions and the value of pH both play important roles during the formation of Au–Ag bimetallic and Au–Ag–Hg trimetallic NRs. In the presence of Hg^{2+}, which has a relatively high reduction potential, we were able to prepare Au–Ag–Hg trimetallic NRs. By controlling the concentration of the added metal ions, which have relatively low reduction potentials, and the pH of the solution, the sizes and shapes of the Au–Ag–Hg trimetallic NRs can be tuned as a result of changes in the reducing ability of ascorbate. The as-prepared NRs possess unique colors and high extinction coefficients, which should be useful for sensing applications after modification with highly selective agents. It is our future goal to develop sensitive and selective color codes for detecting several biomolecules using biofunctional Au–Ag bimetallic and Au–Ag–Hg trimetallic NRs.

Acknowledgements

This work was supported by the National Science Council (NSC 93-2120-M-002-001 and NSC 93-2113-M-002-035) of Taiwan. We thank Mr Ching-Yen Lin and Chih-Yuan Tang in the Instrumentation Center of National Taiwan University for help in conducting the TEM measurements.

Zusing Yang, Yang-Wei Lin, Wei-Lung Tseng and Huan-Tsung Chang*
Department of Chemistry, National Taiwan University, Taipei, Taiwan.
E-mail: changht@ntu.edu.tw; Fax: 011 886 2 23621963;
Tel: 011 886 2 23621963

References

1 (*a*) A. K. Salem, P. C. Searson and K. W. Leong, *Nat. Mater.*, 2003, **2**, 668; (*b*) P. D. Cozzoli, R. Comparelli, E. Fanizza, M. L. Curri, A. Agostiano and D. Laub, *J. Am. Chem. Soc.*, 2004, **126**, 3868; (*c*) B. Nikoobakht and M. A. El-Sayed, *J. Phys. Chem.*

A., 2003, **107**, 3372; (*d*) J. P. Kottmann, O. J. F. Martin, D. R. Smith and S. Schultz, *Chem. Phys. Lett.*, 2001, **341**, 1.
2 (*a*) M. A. El-Sayed, *Acc. Chem. Res.*, 2001, **34**, 257; (*b*) P. E. Marszalek, W. J. Li, H. Greenleaf, A. F. Oberhauser and J. M. Fernandez, *Proc. Natl. Acad. Sci. USA*, 2000, **97**, 6282; (*c*) L.-S. Li, J. Hu, W. Yang and A. P. Alivisatos, *Nano Lett.*, 2001, **1**, 349; (*d*) T. Thurn-Albrecht, J. Schotter, G. A. Kästle, N. Emley, T. Shibauchi, L. Krusin-Elbaum, K. Guarini, C. T. Black, M. T. Tuominen and T. P. Russell, *Science*, 2000, **290**, 2126.
3 (*a*) N. R. Jana, L. Gearheart and C. J. Murphy, *J. Phys. Chem. B.*, 2001, **105**, 4065; (*b*) B. D. Busbee, S. O. Obare and C. J. Murphy, *Adv. Mater.*, 2003, **15**, 414; (*c*) M. Törnblom and U. Henriksson, *J. Phys. Chem. B.*, 1997, **101**, 6028; (*d*) T. Pal, S. De, N. R. Jana, N. Pradhan, R. Mandal, A. Pal, A. E. Beezer and J. C. Mitchell, *Langmuir*, 1998, **14**, 4724.
4 (*a*) S. R. Nicewarner-Peña, R. G. Freeman, B. D. Reiss, L. He, D. J. Peña, I. D. Walton, R. Cromer, C. D. Keating and M. J. Natan, *Science*, 2001, **294**, 137; (*b*) F. Kim, J. H. Song and P. Yang, *J. Am. Chem. Soc.*, 2002, **124**, 14316; (*c*) C. J. Murphy and N. R. Jana, *Adv. Mater.*, 2002, **14**, 80; (*d*) B. Nikoobakht and M. A. El-Sayed, *Chem. Mater.*, 2003, **15**, 1957; (*e*) T. K. Sau and C. J. Murphy, *J. Am. Chem. Soc.*, 2004, **126**, 8648.
5 (*a*) C. S. Ah, S. D. Hong and D.-J. Jang, *J. Phys. Chem. B*, 2001, **105**, 7871; (*b*) M. Liu and P. Guyot-Sionnest, *J. Phys. Chem. B.*, 2004, **108**, 5882; (*c*) M. Moskovits, I. Srnová-Šloufová and B. Vlčková, *J. Chem. Phys.*, 2002, **116**, 10435; (*d*) Y. Mizukoshi, T. Fujimoto, Y. Nagata, R. Oshima and Y. Maeda, *J. Phys. Chem. B.*, 2000, **104**, 6028.
6 (*a*) S. Link, Z. L. Wang and M. A. El-Sayed, *J. Phys. Chem. B.*, 1999, **103**, 3529; (*b*) T. Mokari and U. Banin, *Chem. Mater.*, 2003, **15**, 3955; (*c*) A. Henglein and C. Brancewicz, *Chem. Mater.*, 1997, **9**, 2164; (*d*) T. Shibata, B. A. Bunker, Z. Zhang, D. Meisel, C. F. Vardeman, II and J. D. Gezelter, *J. Am. Chem. Soc.*, 2002, **124**, 11989.
7 (*a*) K. Mallik, M. Mandal, N. Pradhan and T. Pal, *Nano Lett.*, 2001, **1**, 319; (*b*) S.-H. Tsai, Y.-H. Liu, P.-L. Wu and C.-S. Yeh, *J. Mater. Chem.*, 2003, **13**, 978; (*c*) I. Srnová-Šloufová, B. Vlčková, Z. Bastl and T. L. Hasslett, *Langmuir*, 2004, **20**, 3407.
8 (*a*) A. Welch and M. E. van Gemert, *Optical-Thermal Response of Laser-Irradiated Tissue*; Plenum Press: New York, 1995; (*b*) J. J. Storhoff, R. Elghanian, C. A. Mirkin and R. L. Letsinger, *Langmuir*, 2002, **18**, 6666; (*c*) Y. W. Cao, R. Jin and C. A. Mirkin, *J. Am. Chem. Soc.*, 2001, **123**, 7961; (*d*) D. C. Hone, A. H. Haines and D. A. Russell, *Langmuir*, 2003, **19**, 7141.
9 (*a*) N. R. Jana, L. Gearheart and C. J. Murphy, *Chem. Commun.*, 2001, 617; (*b*) S. Chen, Z. L. Wang, J. Ballato, S. H. Foulger and D. L. Carroll, *J. Am. Chem. Soc.*, 2003, **125**, 16186; (*c*) C.-C. Huang, Z. Yang and H.-T. Chang, *Langmuir*, 2004, **20**, 6089; (*d*) Y. Niidome, K. Nishioka, H. Kawasaki and S. Yamada, *Chem. Commun.*, 2003, **18**, 2376.
10 (*a*) B. Nikoobakht and M. A. El-Sayed, *Langmuir*, 2001, **17**, 6368; (*b*) N. R. Jana, L. Gearheart and C. J. Murphy, *Adv. Mater.*, 2003, **13**, 1389; (*c*) Y. G. Sun and Y. N. Xia, *Adv. Mater.*, 2002, **14**, 833; (*d*) Y. Y. Yu, S. S. Chang, C. L. Lee and C. R. C. Wang, *J. Phys. Chem. B*, 1997, **101**, 6661.
11 (*a*) P. L. Gai and M. A. Harmer, *Nano Lett.*, 2002, **2**, 771; (*b*) Z. L. Wang, R. P. Gao, B. Nikoobakht and M. A. El-Sayed, *J. Phys. Chem. B.*, 2000, **104**, 5417; (*c*) M. D. Lay and J. L. Stickney, *J. Am. Chem. Soc.*, 2003, **125**, 1352.
12 (*a*) P. V. Radovanovic and D. R. Gamelin, *J. Am. Chem. Soc.*, 2001, **123**, 12207; (*b*) S. U. Son, Y. Jang, J. Park, H. B. Na, H. M. Park, H. J. Yun, J. Lee and T. Hyeon, *J. Am. Chem. Soc.*, 2004, **126**, 5026; (*c*) C. Zhang, Z. Zhang, B. Yu, J. Shi and X. Zhang, *Anal. Chem.*, 2002, **74**, 96.
13 (*a*) P. Orioli, B. Bruni, M. D. Vaira, L. Messori and F. Piccioli, *Inorg. Chem.*, 2002, **41**, 4312; (*b*) M. M. Taqui Khan and A. E. Martell, *J. Am. Chem. Soc.*, 1968, **90**, 6011; (*c*) M. M. Taqui Khan and A. E. Martell, *J. Am. Chem. Soc.*, 1968, **90**, 3386; (*d*) M. M. Taqui Khan and A. E. Martell, *J. Am. Chem. Soc.*, 1967, **89**, 4176; (*e*) S. Kotrly and L. Sucha, *Handbook of Chemical Equilibria in Analytical Chemistry*; Halsted Press, New York, 1985.
14 (*a*) T. Morris, H. Copeland, E. McLinden, S. Wilson and G. Szulczewski, *Langmuir*, 2002, **18**, 7261; (*b*) A. Henglein and M. Giersig, *J. Phys. Chem. B.*, 2000, **104**, 5056; (*c*) L. Katsikas, M. Gutiérrez and A. Henglein, *J. Phys. Chem.*, 1996, **100**, 11203.
15 *Handbook of Chemistry and Physics*, ed. D. R. Lide, CRC Press, New York, 76th edn., 1995, pp. 121–140.
16 For glycine (L), the stability constants are log $K(Fe^{3+})$ = 10.8 (FeL), log $K(Co^{2+})$ = 5.1 (CoL), log $K(Hg^{2+})$ = 10.9 (HgL), and log $K(Hg^{2+})$ = 20.1 (HgL_2). See: F. M. M. Morel, *Principles of Aquatic Chemistry*; Wiley-Interscience: New York, 1983, pp. 237–310.

